Vitamin K3 derivative induces apoptotic cell death in neuroblastoma via downregulation of MYCN expression

Hiroyuki Yoda[a,*], Toshimitsu Nakayama[b], Motofumi Miura[c], Masaharu Toriyama[c], Shigeyasu Motohashi[c], Takashi Suzuki[a,d]

[a] *Laboratory of Clinical Medicine, School of Pharmacy, Nihon University, 7-7-1 Narashinodai, Funabashi, Chiba, 274-8555, Japan*
[b] *Center for Pharmacist Education, School of Pharmacy, Nihon University, 7-7-1 Narashinodai, Funabashi, Chiba, 274-8555, Japan*
[c] *Laboratory of Molecular Chemistry, School of Pharmacy, Nihon University, 7-7-1 Narashinodai, Funabashi, Chiba, 274-8555, Japan*
[d] *Department of Pediatrics and Child Health, School of Medicine, Nihon University, 30-1 Oyaguchikami, Itabashi-ku, Tokyo, 173-0032, Japan*

ARTICLE INFO

ABSTRACT

Neuroblastoma is a pediatric malignant tumor arising from the sympathetic nervous system. The patients with high-risk neuroblastomas frequently exhibit amplification and high expression of the MYCN gene, resulting in worse clinical outcomes. Vitamin K3 (VK3) is a synthetic VK-like compound that has been known to have antitumor activity against various types of cancers. In the present study, we have asked whether VK3 and its derivative, VK3-OH, could have the antitumor activity against neuroblastoma-derived cells. Based on our results, VK3-OH strongly inhibited cell proliferation and induced apoptotic cell death compared to VK3. Treatment of MYCN-driven neuroblastoma cells with VK3-OH potentiated tumor suppressor p53 accompanied by down-regulation of anti-apoptotic Bcl-2 and Mcl-1. Interestingly, VK3-OH also suppressed the MYCN at mRNA and protein levels. Furthermore, we found downregulation of LIN28B following VK3-OH treatment in *MYCN*-amplified and overexpressed neuroblastoma cells. Collectively, our current findings strongly suggest that VK3-OH provides a potential therapeutic strategy for patients with MYCN-driven neuroblastomas.

1. Introduction

Neuroblastoma is a rare solid tumor arising from the peripheral sympathetic nervous system occurring in infancy and early childhood showing the various clinical features such as spontaneous regression and lethality [1,2]. MYCN is a highly pleiotropic transcription factor associated with the diverse cellular processes and acts as a driver gene in neuroblastoma [3,4]. Advancements in the therapy for patients with the high-risk neuroblastoma accompanied by the enhanced MYCN expression caused by gene amplification have improved 5-year overall survival rate to 50%, yet the high-dose combination chemotherapy is generally used [5,6]. However, a study on patients with high-risk neuroblastoma who have survived, indicative of a high prevalence of late effects, including second malignancy, growth failure, and fertility [7]. To overcome these difficulties, new treatment approaches with reduced late effects are required.

The synthetic chemical compound vitamin K3 (VK3), also known as menadione, has been known to have anticancer activity against various types of adult cancer cells [8–10], compared to the natural compounds such as VK1 and VK2 [11]. In particular, VK3 analogs with the short thioether side chains exhibit the potential cell growth inhibition ability in several malignant tumor cells [12]. These observations prompted us to design and synthesize seven VK3 analogs with the thioether side chains, and then we have examined whether they could have the anticancer activity against human neuroblastoma-derived cells. To date, we have reported that 3-(1,4-dihydro-3-methyl-1,4-dioxo-2-naphtylthio)propanoic acid (VK3-COOH) augments the cellular differentiation through the regulation of gene expressions of *c-fos* and *GAP-43* in neuroblastoma cells [13]. Additionally, 2-[(2-methoxy)ethylthio]-3-methyl-1,4-naphthoquinone (VK3-OCH$_3$) exhibits the selective anticancer activity against human neuroblastoma cells via overexpression of heme oxygenase-1 [14]. Among these VK3 analogs, we have found that 2-[(2-hydroxy)ethylthio]-3-methyl-1,4-naphthoquinone (VK3-OH) strongly attenuates the proliferation of neuroblastoma cells. However, little is known about precise pharmacological mechanisms by which VK3 analog, VK3-OH, could induce cell death in neuroblastoma. In this study, we investigated the molecular mechanisms underlying VK3-OH-induced cell death in neuroblastoma cells.

* Corresponding author. Present address: Division of Innovative Cancer Therapeutics, Chiba Cancer Center Research Institute, 666-2 Nitona, Chuo-ku, Chiba, 260–8717, Japan.

E-mail address: hyoda@chiba-cc.jp (H. Yoda).

2. Materials and methods

2.1. Compounds

VK3 and cisplatin (CDDP) were purchased from Wako (Osaka, Japan). VK3 derivative (VK3-OH) was synthesized as described previously [13].

2.2. Cells

Human neuroblastoma CHP134, Kelly, SK-N-BE(2), SH-SY5Y, SK-N-AS, and SK-N-SH cells were obtained from ECACC, and IMR32 cells were obtained from RIKEN Cell Bank (Ibaraki, Japan). SHEP21N cells were kindly gifted from Dr. Manfred Schwab. Human embryonic kidney (HEK) 293 cells were obtained from ATCC. These cells were cultured in RPMI-1640 medium supplemented with 100 U/mL penicillin, 100 μg/mL streptomycin, and 10% heat-inactivated fetal bovine serum (Thermo Fisher Scientific, Waltham, MA). All cells were cultured at 37 °C under 5% CO_2 and tested negative for *Mycoplasma* contamination using TaKaRa PCR Mycoplasma Detection Set (Takara Bio, Shiga, Japan).

2.3. WST-8 cell proliferation assay

Cells were seeded on 96-well culture plate and incubated for 24 h. After treatment with VK3 or VK3-OH for 48 h, the absorbance of WST-8 formazan (Dojindo, Kumamoto, Japan) was measured by a microplate reader (Corona, Ibaraki, Japan). The cell proliferation rate and IC_{50} values were calculated as the percentage of that of the DMSO control.

2.4. Cell cycle analysis

Cells were seeded on 6-well culture plate and incubated for 24 h. After treatment with VK3 or VK3-OH for 24 h, cells were collected and washed in PBS. After the fixation with 70% ethanol, cells were treated with RNase A and propidium iodide for 30 min under dark condition and analyzed by BD FACSCalibur (BD, Franklin Lakes, NJ). The analysis was conducted using FlowJo Software (BD).

2.5. Live/dead viability/cytotoxicity assay

Cells were seeded on 6-well culture plate and incubated for 24 h. After treatment with VK3, VK3-OH, or CDDP for 24 h, cells were collected and washed in PBS. Cells were then subjected to Live/Dead viability/cytotoxicity assay according to the manufacturer's instructions (Thermo Fisher Scientific). Cells were analyzed by a cytomics FC500 (Beckman Coulter, Fullerton, CA).

2.6. Hoechst 33342 staining

Cells were seeded on 6-well culture plate and incubated for 24 h. After treatment with VK3, VK3-OH, or CDDP for 24 h, cells were stained with Hoechst 33342 solution (Wako) and incubated for 15 min. The stained cell nuclei were visualized using a fluorescence microscope IX71 (Olympus, Tokyo, Japan).

2.7. Western blot analysis

Cells were seeded on 6-well culture plates and incubated for 24 h. After treatment with VK3 or VK3-OH for 0–24 h, cells were collected, washed in PBS and lysed in RIPA buffer containing protease inhibitor and phosphatase inhibitor (Roche Diagnostics, Mannheim, Germany). Samples were separated by TGX Stain-Free FastCast Acrylamide (Bio-Rad, Hercules, CA) and transferred onto Immobilon-P PVDF transfer membrane (Merck, Darmstadt, Germany) using Trans-Blot Turbo Blotting System (Bio-Rad). After blocking with 5% Difco Skim Milk (BD) for 1 h, the membranes were probed overnight with the primary antibodies at 4 °C. The membranes were washed in TBS-T and incubated with the appropriate secondary antibodies at room temperature for 1 h. The protein bands were visualized by ECL Prime Western Blotting Detection Reagent and ImageQuant LAS 4000mini system (GE Healthcare, Chicago, IL). Antibodies used were as follows: anti-poly (ADP-ribose)polymerase (PARP; Cell Signaling Technology (CST), Danvers, MA), anti-cleaved caspase-3 (CST), anti-p53 (Santa Cruz Biotechnology, Dallas, TX), anti-phosphorylated p53 at Ser15 (CST), anti-Bcl-2 (CST), anti-Bcl-xL (CST), anti-Mcl-1 (Santa Cruz Biotechnology), anti-N-MYC (CST), anti-LIN28B (CST), anti-β-tubulin (CST), anti-mouse IgG, HRP-linked antibody (CST), and anti-rabbit IgG, HRP-linked antibody (CST).

2.8. Crystal violet staining

Cells were seeded on 6-well culture plate and incubated for 24 h. After treatment with VK3-OH for 24 h, cells were washed in PBS, fixed in 4% paraformaldehyde for 30 min and stained with 0.2% crystal violet solution.

2.9. qPCR analysis

Cells were seeded on 6-well culture plate for 24 h. After treatment with VK3 or VK3-OH for 6 h, cells were collected and washed in PBS, and RNA was extracted using RNeasy Plus Mini Kit (Qiagen, Hilden, Germany) according to the manufacturer's instructions. cDNA was synthesized using SuperScript VILO Master Mix (Thermo Fisher Scientific) according to the manufacturer's protocols. Reactions were carried out using an Applied Biosystems PowerUp SYBR Green Master Mix and a StepOne Plus Real-Time PCR (Thermo Fisher Scientific). Primer sequences used were as follows: *MYCN*, 5′ − GGACACCCTGAG CGATTCAGA − 3′ and 5′ − AGGAGGAACGCCGCTTCT − 3′; *LIN28B*, 5′ − CCTTGGATATTCCAGTCGATGT − 3′ and 5′ − TGACTCAAGGCCTTTGG AAG − 3′; *GAPDH*, 5′ − CGACCACTTTGTCAAGCTCA − 3′ and 5′ − AGG GGTCTACATGGCAACTG − 3′.

2.10. Statistical analysis

Data were represented as mean ± S.D. (n = 3). Significance was determined using one-way analysis of variance (ANOVA) followed by either Bonferroni's test for comparing three or more data points or Student's t-test when comparing two data points. All analysis was performed using Graph Pad Prism 7.0 (GraphPad Software, Lajolla, CA). Protein band intensities were quantified by NIH ImageJ software. *P*-values < 0.05 were considered statistically significant.

3. Results

3.1. VK3 and VK3-OH inhibit the proliferation of neuroblastoma cells

To evaluate the anticancer effects of VK3 and VK3-OH on neuroblastoma cells (Supplementary Fig. S1A), we have employed seven human neuroblastoma cells and performed cell proliferation assay. After exposure to varying concentrations of VK3 or VK3-OH for 48 h, both compounds prohibited the proliferation of all neuroblastoma cells. The median IC_{50} values of VK3 and VK3-OH were 7.0 μM and 2.4 μM, respectively (Fig. 1A). Similarly, non-cancerous HEK293 cells were sensitive to both compounds (Supplementary Fig. S1B). We next checked the effects of VK3 and VK3-OH on cell cycle progression of both compounds-treated IMR32 cells with *MYCN* amplification. To this end, IMR32 cells were exposed to both compounds for 24 h. As shown in Fig. 1B and Supplementary Fig. S1C, the number of cells arrested at the G_2/M phase was increased in a dose-dependent manner.

A

Cell lines	VK3 (µM)	VK3-OH (µM)
CHP134	3.0	0.6
IMR32	4.9	1.5
Kelly	9.1	1.9
SH-SY5Y	3.5	2.7
SK-N-AS	11.0	3.0
SK-N-BE(2)	8.6	2.4
SK-N-SH	7.0	10.7

B
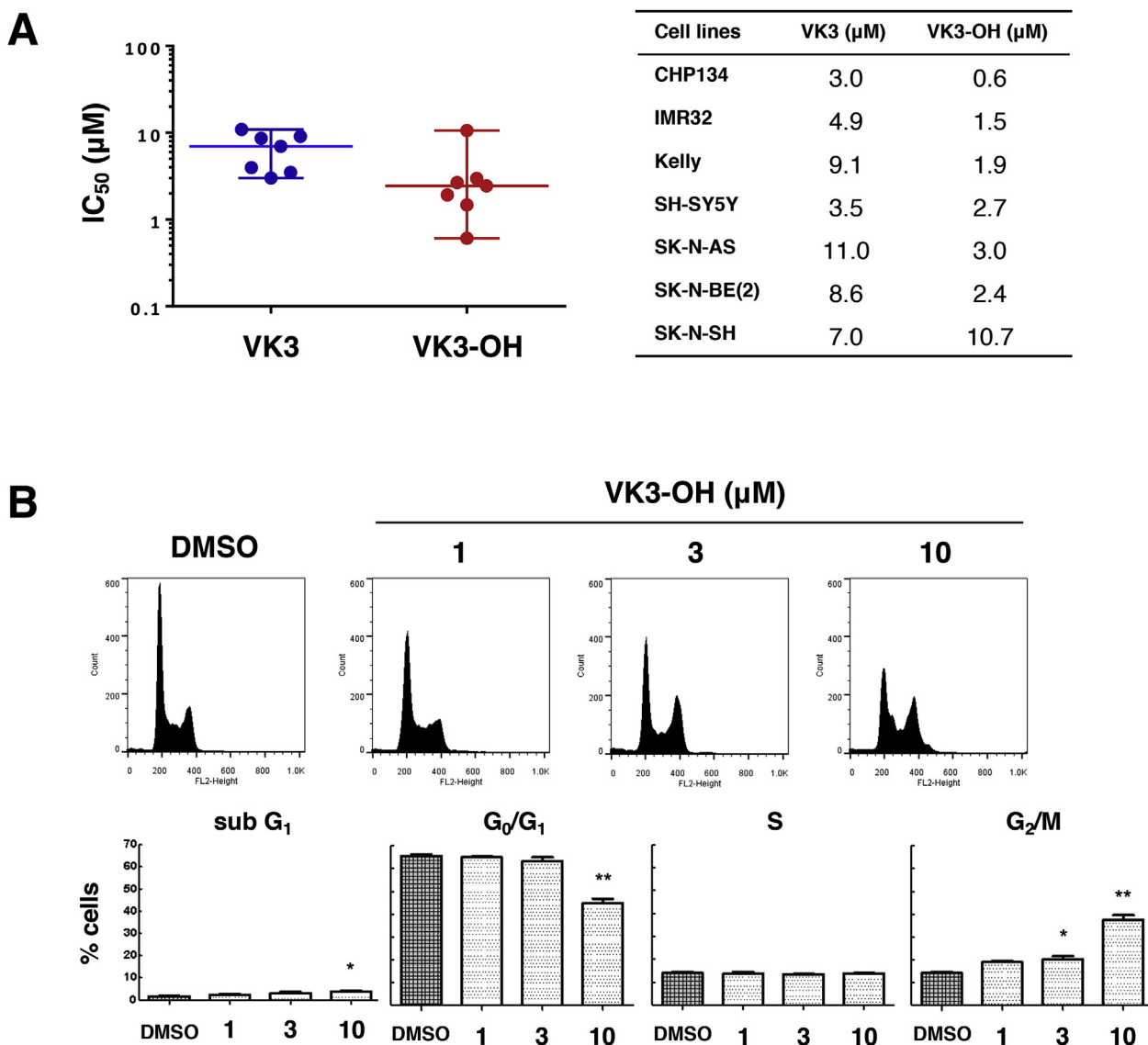
Fig. 1. VK3 and VK3-OH inhibit cell proliferation of neuroblastoma cells.
(A) After treatment with VK3 or VK3 derivative (VK3-OH) for 48 h, IC_{50} values were determined by WST-8 cell proliferation assay. Each plot showed neuroblastoma-derived cells, and the horizontal line indicated the median values of IC_{50}.
(B) After treatment with VK3-OH for 24 h, cell cycle distributions were determined by flow cytometry. The representative histograms showed the cell cycle distributions of IMR32 cells (top). Each column indicated the cell ratio (bottom). Data represented the mean ± SD of three independent experiments (*$P < 0.05$, **$P < 0.01$). DMSO was used as a control.

3.2. VK3-OH induces apoptotic cell death in IMR32 neuroblastoma cells

To further confirm the inhibitory effects of VK-3 and VK3-OH on neuroblastoma cells, we analyzed their cytotoxic effects on IMR32 cells by Live/Dead viability/cytotoxicity assay. After 24 h of VK3-OH treatment, the number of ethidium homodimer-1-positive cells (dead cells) was significantly increased, whereas the number of calcein AM-positive cells (live cells) was decreased, suggesting that VK3-OH impaired the cell membrane integrity and the activity of intracellular esterase (Fig. 2A). We next examined the morphological changes of IMR32 cells following VK3-OH treatment. Representative images of Hoechst 33342 staining demonstrated that obvious morphological changes accompanied by properties of apoptotic cell death, such as cell shrinking, chromatin condensation, and nuclear fragmentation, take place (Fig. 2B). We have also obtained similar results in IMR32 cells treated with VK3 or with CDDP (Supplementary Fig. S2).

3.3. VK3-OH promotes p53-mediated cell death in IMR32 and MYCN-expressing SHEP21N neuroblastoma cells

To elucidate precise molecular mechanisms behind cell death following VK3 and VK3-OH treatment in neuroblastoma cells, we have compared the amounts of cleaved caspase-3 and PARP, which are representative apoptotic cell death markers, by Western blot analysis (Fig. 3A). Since VK3 and VK3-OH-treated IMR32 cells showed the elevated amounts of the above-mentioned cleaved materials, we selected VK3-OH as the lead compound and utilized for further experiments. IMR32 cells were exposed to 10 µM of VK3-OH. At the indicated time points after the treatment, cell lysates were analyzed for p53 and p53-related gene products by Western blot analysis. As seen in Fig. 3B, VK3-OH treatment induced the phosphorylation of p53 at Ser-15, and elevated the expression of p53-target gene product $p21^{WAF1}$. Similarly, the amounts of cleaved caspase-3 and PARP were increased in response to VK3-OH. Furthermore, VK3-OH decreased the expression of anti-apoptotic Bcl-2 and Mcl-1.
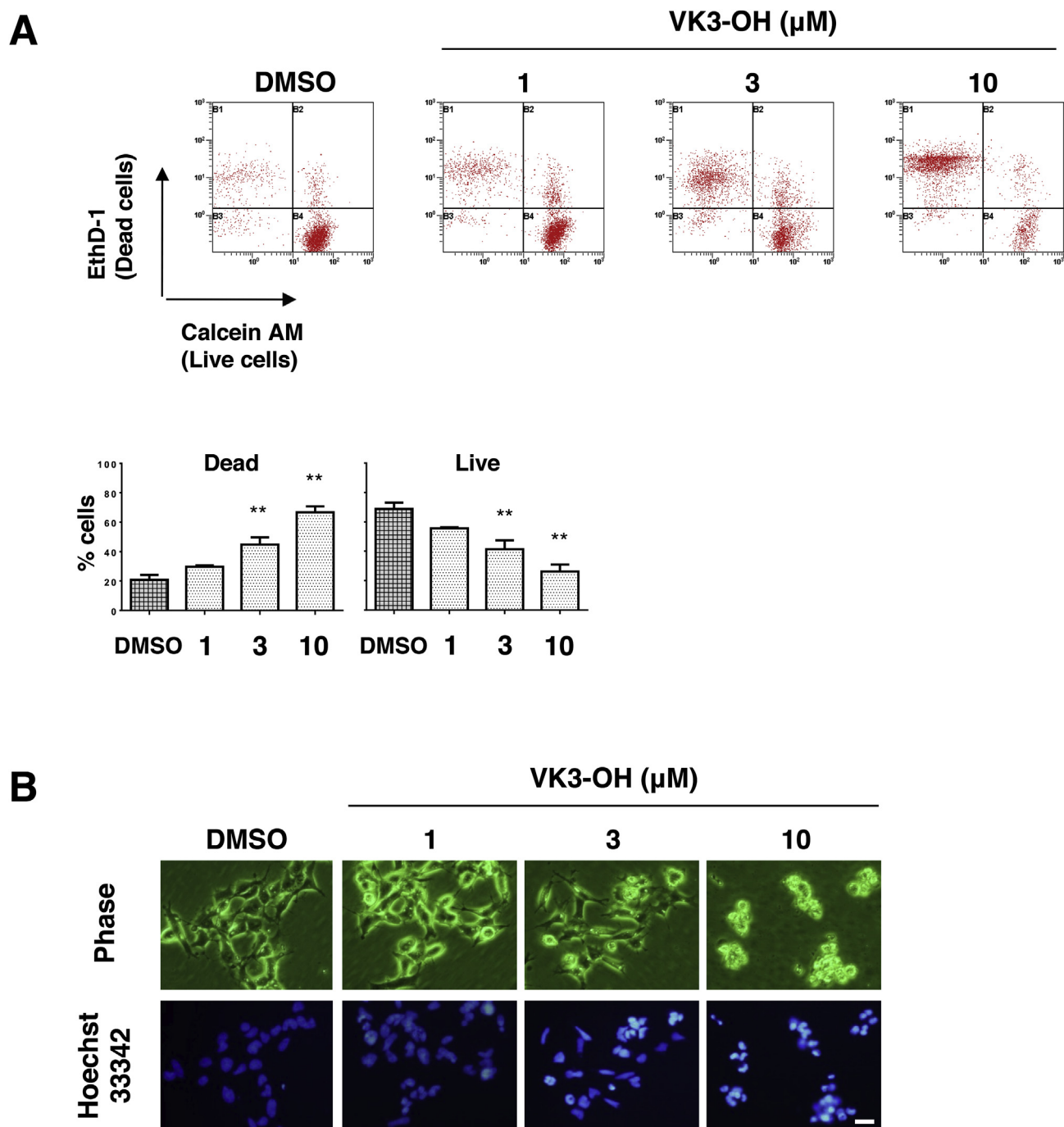
Fig. 2. VK3-OH induces cell death in neuroblastoma cells.
(A) IMR32 cells were treated with VK3-OH. Twenty-four hours after treatment, live cells and dead cells were identified by LIVE/DEAD cell viability assay. Representative images showed the results of the assay. Ethidium homodimer-1 (EthD-1)-positive and calcein AM-positive indicated dead cells and live cells, respectively (top). Each column showed the cell ratio. Data represented the mean ± SD of three independent experiments (bottom; *P < 0.05, **P < 0.01). DMSO was used as a control.
(B) IMR32 cells were treated with the indicated concentrations of VK3-OH. Twenty-four hours after treatment, cells were treated with Hoechst 33342. Representative phase-contrast images (top) and fluorescence images (bottom) of IMR32 cells were taken. DMSO was used as a control. Bar, 20 μm.

To verify the effects of MYCN on the sensitivity to VK3-OH, we have employed SHEP21N neuroblastoma cells in which MYCN was inducible. As shown in Fig. 3C and D, VK3-OH showed similar cytotoxic effects on SHEP21N cells regardless of MYCN expression. Western blot analysis revealed that the accumulation of phosphorylated p53 at Ser-15, p21^{WAF1}, and DNA damage marker γH2AX was detectable in MYCN-expressing SHEP21N cells treated with VK3-OH. Additionally, VK3-OH treatment downregulated Bcl-2 and Mcl-1 in MYCN-expressing

SHEP21N cells following VK3-OH exposure (Fig. 3E). However, VK3-OH-mediated induction of cleaved PARP was undetectable in SHEP21N cells regardless of MYCN.

3.4. VK3-OH suppresses MYCN and LIN28B in MYCN-driven neuroblastoma cells

As described above, Bcl-2 and Mcl-1 were reduced in VK3-OH-
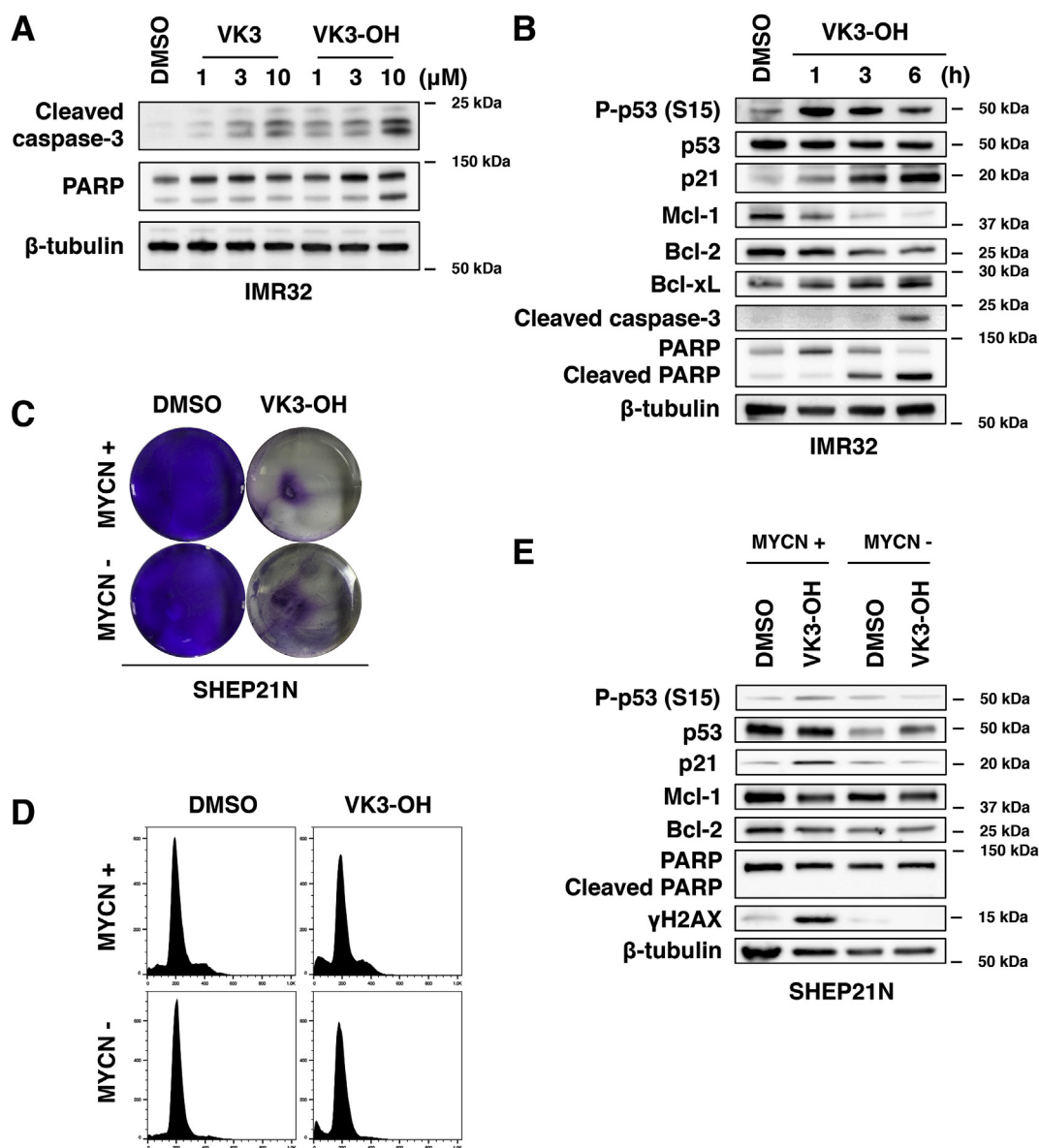
Fig. 3. VK3-OH potentiates p53-mediated apoptotic cell death of neuroblastoma cells.
(A) IMR32 cells were treated with the indicated concentrations of VK3 or with VK3-OH. Twenty-four hours after treatment, cell lysates were prepared and analyzed for cleaved caspase-3 and PARP by Western blot analysis.
(B) IMR32 cells were treated with VK3-OH (10 μM). At the indicated time periods after treatment, cell lysates were prepared and analyzed for p53 and p53-related gene products by Western blot analysis.
(C) After treatment with VK3-OH (10 μM) for 24 h, MYCN-inducible SHEP21N cells with or without MYCN overexpression were stained with crystal violet.
(D) Cell cycle distributions of SHEP21N cells with or without MYCN overexpression were determined by flow cytometry.
(E) SHEP21N cells were treated with DMSO or with VK3-OH (10 μM). Six hours after the treatment, cell lysates were prepared and analyzed for the indicated proteins by Western blot analysis. DMSO was used as a control. β-tubulin was used as a loading control.

treated IMR32 and MYCN-expressing SHEP21N cells. Of note, over-expression of MYCN has been shown to attenuate apoptotic cell death of neuroblastoma [3,4], raising a possibility that VK3-OH could regulate MYCN expression. To check this possibility, we sought to determine the MYCN at mRNA and protein levels in SHEP21N cells by qPCR and Western blot analysis. Interestingly, VK3-OH markedly reduced the MYCN at mRNA and protein levels in SHEP21N cells (Fig. 4A and B).

Since it has been shown that LIN28B regulates MYCN at the post-transcriptional level via *let*-7 miRNA in neuroblastoma [15], we sought to examine the expression level of LIN28B in SHEP21N cells. As seen in Fig. 4A and C, VK3-OH treatment decreased the LIN28B expression level in SHEP21N cells. We have also validated the expression levels of MYCN and LIN28B in *MYCN*-amplified neuroblastoma cells as well as

SHEP21N cells (Fig. 4D − F). Together, our results indicate that VK3-OH prohibits MYCN expression through the suppression of LIN28B at the post-transcriptional level.

4. Discussion

VK is an essential nutrient that plays an important role in blood coagulation through post-translational modifications to clotting factors. VK is also known to act as a cofactor for the enzyme γ-glutamyl car-boxylase, which catalyzes the γ-carboxylation of glutamate residues of vitamin K-dependent proteins [16]. Recent studies suggest that VK and its derivatives link to the cell proliferation of neural stem cells and the differentiation of the neuronal progenitor cells [17,18]. However, the
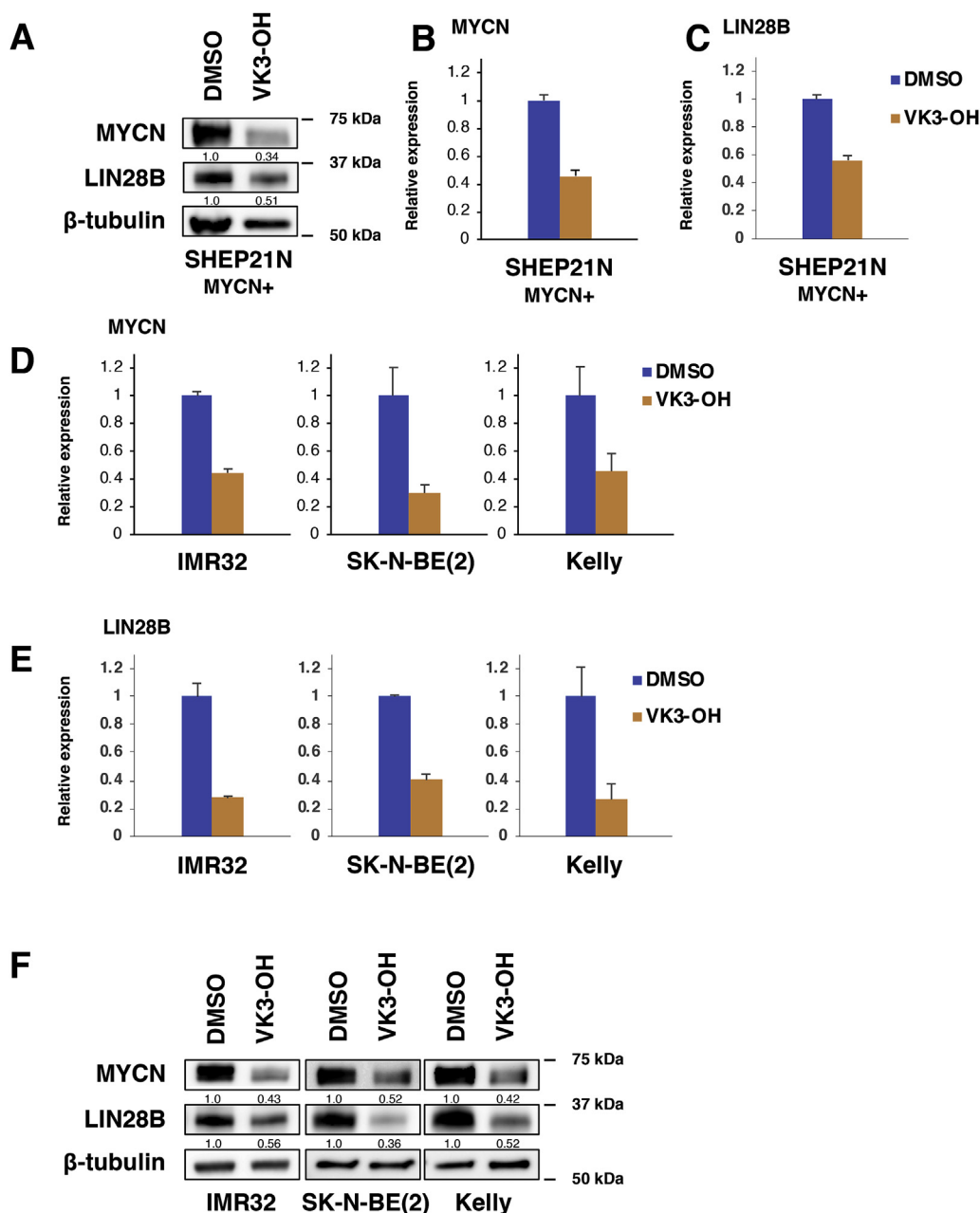
Fig. 4. VK3-OH downregulates MYCN in neuroblastoma cells.

(A–C) MYCN-overexpressing SHEP21N cells were treated with VK3-OH (10 μM). Six hours after the exposure, cell lysates and total RNA were extracted and analyzed for MYCN as well as LIN28B by Western blot analysis (A) and qPCR (B and C), respectively. DMSO was used as a control. β-tubulin and *GAPDH* were used as a loading control and internal control, respectively.

(D and E) Under the same conditions, total RNA was prepared from *MYCN*-amplified IMR32, SK-N-BE(2), and Kelly cells and analyzed for *MYCN* (D) and *LIN28B* (E) by qPCR. DMSO was used as a control. *GAPDH* was used as an internal control.

(F) Under the same conditions, cell lysates were prepared from *MYCN*-amplified IMR32, SK-N-BE(2), and Kelly cells and analyzed for MYCN and LIN28B by Western blot analysis. DMSO was used as a control. β-tubulin and *GAPDH* were used as an internal control and loading control, respectively.

biological significance of VK and its role in the development/progression of cancer, including neuroblastoma, have been elusive.

In this study, we have revealed that VK3 analog, VK3-OH, has an antitumor effect on neuroblastoma cells. Based on our present results, VK3-OH caused a decrease in cell proliferation, cell cycle progression, and induced apoptotic cell death via p53 activation. Additionally, VK3-OH prohibited MYCN/LIN28B expression accompanied by the downregulation of Bcl-2 and Mcl-1 in neuroblastoma cells. Our current observations demonstrated that the IC$_{50}$ value of VK3-OH is approximately three times lower than that of non-modified VK3, and the cell cycle is arrested at the G$_2$/M phase following VK3-OH treatment in neuroblastoma cells. According to the previous reports, the presence of the side chain, especially thioether VK3 adducts, enhanced the cellular cytotoxicity, which might be due to the unexpected reactivity to cysteine of proteins [12,19] and the direct inhibition of Cdc25 phosphatase [20,21], which regulates the G$_2$/M phase transition [22].

Since MYCN silencing is a lethal event for MYCN-addicted neuroblastomas [23,24], several promising approaches to target the pro-

oncogenic MYCN pathway have been under development [25–29]. VK3-OH led to a marked increase in apoptotic cell death accompanied by the cleavage of caspase-3 and PARP and phosphorylated p53 at Ser-15. In addition, VK3-OH promoted a decrease in the expression levels of anti-apoptotic factors such as Bcl-2 and Mcl-1, in IMR32 and/or MYCN-expressing SHEP21N cells. In a good agreement with our results, the recent studies have shown that the small chemical compound-mediated inhibition of Bcl-2 and/or Mcl-1 induces apoptosis, which might be an attractive therapeutic approach for the patients bearing neuroblastoma with or without *MYCN* amplification [30,31]. It has been described that VK3 also generates reactive oxygen species (ROS), and the higher level of ROS triggers apoptotic cell death [32]. Indeed, γH2AX was detected following VK3-OH treatment in MYCN-expressing SHEP21N cells. However, we did not detect ROS production under our experimental conditions (Supplementary Fig. S3), indicating that VK3-OH might trigger apoptotic cell death through the other mechanisms.

Our present findings also demonstrated that MYCN is downregulated at mRNA and protein levels in *MYCN*-amplified

neuroblastoma cells in response to VK3-OH. Interestingly, this observation was also obtained in MYCN-induced SHEP21N cells that lacked the canonical binding sites of transcription factors within the *MYCN* promoter region [33]. To identify a distinct molecular mechanism behind *MYCN* transcription, we have employed BET bromodomain inhibitor JQ1, which suppressed *MYCN* transcription of neuroblastoma cells [34]. However, JQ1 failed to reduce the *MYCN* mRNA level in SHEP21N cells (Supplementary Fig. S4), suggesting that VK3-OH-induced MYCN suppression might be regulated at post-transcriptional levels. In support of this possibility, VK3-OH decreased LIN28B expression. LIN28B has been shown to destabilize *MYCN* mRNA via regulating *let*-7 miRNA [15]. Although further study should be required to identify the molecular mechanisms of how VK3-OH could cause the suppression of MYCN, our findings imply that VK3-OH might regulate MYCN/LIN28B axis, and thereby promoting apoptotic cell death in *MYCN*-amplified as well as MYCN-overexpressing neuroblastoma cells. Taken together, our current results strongly suggest that VK3-OH-mediated dysregulation of MYCN regulatory machinery plays a vital role in the induction of apoptotic cell death in neuroblastoma cells.

In summary, VK3-OH is a potential therapeutic agent for the high-risk neuroblastoma with gene amplification and/or overexpression of MYCN.

Declaration of competing interest

There are no conflicts of interest.

Acknowledgements

Appendix A. Supplementary data

Supplementary data to this article can be found online at https://doi.org/10.1016/j.bbrep.2019.100701.

Transparency document

Transparency document related to this article can be found online at https://doi.org/10.1016/j.bbrep.2019.100701.

References

[1] K.K. Matthay, J.M. Maris, G. Schleiermacher, A. Nakagawara, C.L. Mackall, L. Diller, W.A. Weiss, Neuroblastoma, nature reviews, Dis. Prim. 2 (2016) 16078, https://doi.org/10.1038/nrdp.2016.78.

[2] G.M. Brodeur, R. Bagatell, Mechanisms of neuroblastoma regression, Nat. Rev. Clin. Oncol. 11 (2014) 704–713, https://doi.org/10.1038/nrclinonc.2014.168.

[3] D.S. Rickman, J.H. Schulte, M. Eilers, The expanding world of N-MYC-Driven tumors, Canc. Discov. 8 (2018) 150–163, https://doi.org/10.1158/2159-8290.Cd-17-0273.

[4] M. Huang, W.A. Weiss, Neuroblastoma and MYCN, Cold Spring Harbor Perspect. Med. 3 (2013) a014415, https://doi.org/10.1101/cshperspect.a014415.

[5] N.R. Pinto, M.A. Applebaum, S.L. Volchenboum, K.K. Matthay, W.B. London, P.F. Ambros, A. Nakagawara, F. Berthold, G. Schleiermacher, J.R. Park, D. Valteau-Couanet, A.D. Pearson, S.L. Cohn, Advances in risk classification and treatment strategies for neuroblastoma, J. Clin. Oncol. Off. J. Am. Soc. Clin. Oncol. 33 (2015) 3008–3017, https://doi.org/10.1200/jco.2014.59.4648.

[6] S.L. Cohn, A.D. Pearson, W.B. London, T. Monclair, P.F. Ambros, G.M. Brodeur, A. Faldum, B. Hero, T. Iehara, D. Machin, V. Mosseri, T. Simon, A. Garaventa, V. Castel, K.K. Matthay, The international neuroblastoma risk group (INRG) classification system: an INRG task force report, J. Clin. Oncol. Off. J. Am. Soc. Clin. Oncol. 27 (2009) 289–297, https://doi.org/10.1200/jco.2008.16.6785.

[7] M.A. Applebaum, Z. Vaksman, S.M. Lee, E.A. Hungate, T.O. Henderson, W.B. London, N. Pinto, S.L. Volchenboum, J.R. Park, A. Naranjo, B. Hero, A.D. Pearson, B.E. Stranger, S.L. Cohn, S.J. Diskin, Neuroblastoma survivors are at increased risk for second malignancies: a report from the International Neuroblastoma Risk Group Project, Eur. J. Cancer (Oxford, England : 1990) 72

[8] F.Y. Wu, T.P. Sun, Vitamin K3 induces cell cycle arrest and cell death by inhibiting Cdc25 phosphatase, Eur. J. Cancer (Oxford, England : 1990) 35 (1999) 1388–1393.

[9] F.Y. Wu, N.T. Chang, W.J. Chen, C.C. Juan, Vitamin K3-induced cell cycle arrest and apoptotic cell death are accompanied by altered expression of c-fos and c-myc in nasopharyngeal carcinoma cells, Oncogene 8 (1993) 2237–2244.

[10] L.M. Nutter, A.L. Cheng, H.L. Hung, R.K. Hsieh, E.O. Ngo, T.W. Liu, Menadione: spectrum of anticancer activity and effects on nucleotide metabolism in human neoplastic cell lines, Biochem. Pharmacol. 41 (1991) 1283–1292.

[11] R. Sasaki, Y. Suzuki, Y. Yonezawa, Y. Ota, Y. Okamoto, Y. Demizu, P. Huang, H. Yoshida, K. Sugimura, Y. Mizushina, DNA polymerase gamma inhibition by vitamin K3 induces mitochondria-mediated cytotoxicity in human cancer cells, Cancer Sci. 99 (2008) 1040–1048, https://doi.org/10.1111/j.1349-7006.2008.00771.x.

[12] Y. Nishikawa, B.I. Carr, M. Wang, S. Kar, F. Finn, P. Dowd, Z.B. Zheng, J. Kerns, S. Naganathan, Growth inhibition of hepatoma cells induced by vitamin K and its analogs, J. Biol. Chem. 270 (1995) 28304–28310.

[13] T. Nakayama, S. Asami, S. Ono, M. Miura, M. Hayasaka, Y. Yoshida, M. Toriyama, S. Motohashi, T. Suzuki, Effect of cell differentiation for neuroblastoma by vitamin k analogs, Jpn. J. Clin. Oncol. 39 (2009) 251–259, https://doi.org/10.1093/jjco/hyp011.

[14] T. Kitano, H. Yoda, K. Tabata, M. Miura, M. Toriyama, S. Motohashi, T. Suzuki, Vitamin K3 analogs induce selective tumor cytotoxicity in neuroblastoma, Biol. Pharm. Bull. 35 (2012) 617–623.

[15] J.J. Molenaar, R. Domingo-Fernandez, M.E. Ebus, S. Lindner, J. Koster, K. Drabek, P. Mestdagh, P. van Sluis, L.J. Valentijn, J. van Nes, M. Broekmans, F. Haneveld, R. Volckmann, I. Bray, L. Heukamp, A. Sprussel, T. Thor, K. Kieckbusch, L. Klein-Hitpass, M. Fischer, J. Vandesompele, A. Schramm, M.M. van Noesel, L. Varesio, F. Speleman, A. Eggert, R.L. Stallings, H.N. Caron, R. Versteeg, J.H. Schulte, LIN28B induces neuroblastoma and enhances MYCN levels via let-7 suppression, Nat. Genet. 44 (2012) 1199–1206, https://doi.org/10.1038/ng.2436.

[16] Y. Hirota, Y. Suhara, New aspects of vitamin K Research with synthetic ligands: transcriptional activity via SXR and neural differentiation activity, Int. J. Mol. Sci. 20 (2019), https://doi.org/10.3390/ijms20123006.

[17] R. Sakane, K. Kimura, Y. Hirota, M. Ishizawa, Y. Takagi, A. Wada, S. Kuwahara, M. Makishima, Y. Suhara, Synthesis of novel vitamin K derivatives with alkylated phenyl groups introduced at the omega-terminal side chain and evaluation of their neural differentiation activities, Bioorg. Med. Chem. Lett 27 (2017) 4881–4884, https://doi.org/10.1016/j.bmcl.2017.09.038.

[18] A. Gely-Pernot, V. Coronas, T. Harnois, L. Prestoz, N. Mandairon, A. Didier, J.M. Berjeaud, A. Monvoisin, N. Bourmeyster, P.G. De Frutos, M. Philippe, O. Benzakour, An endogenous vitamin K-dependent mechanism regulates cell proliferation in the brain subventricular stem cell niche, Stem Cells 30 (2012) 719–731, https://doi.org/10.1002/stem.1045.

[19] W.W. Li, J. Heinze, W. Haehnel, Site-specific binding of quinones to proteins through thiol addition and addition-elimination reactions, J. Am. Chem. Soc. 127 (2005) 6140–6141, https://doi.org/10.1021/ja050974x.

[20] S. Kar, I.M. Lefterov, M. Wang, J.S. Lazo, C.N. Scott, C.S. Wilcox, B.I. Carr, Binding and inhibition of Cdc25 phosphatases by vitamin K analogues, Biochemistry 42 (2003) 10490–10497, https://doi.org/10.1021/bi027418p.

[21] K. Tamura, E.C. Southwick, J. Kerns, K. Rosi, B.I. Carr, C. Wilcox, J.S. Lazo, Cdc25 inhibition and cell cycle arrest by a synthetic thioalkyl vitamin K analogue, Cancer Res. 60 (2000) 1317–1325.

[22] R. Boutros, V. Lobjois, B. Ducommun, CDC25 phosphatases in cancer cells: key players? Good targets? Nat. Rev. Cancer 7 (2007) 495–507, https://doi.org/10.1038/nrc2169.

[23] R. Jiang, S. Xue, Z. Jin, Stable knockdown of MYCN by lentivirus-based RNAi inhibits human neuroblastoma cells growth in vitro and in vivo, Biochem. Biophys. Res. Commun. 410 (2011) 364–370, https://doi.org/10.1016/j.bbrc.2011.06.020.

[24] J.H. Kang, P.G. Rychahou, T.A. Ishola, J. Qiao, B.M. Evers, D.H. Chung, MYCN silencing induces differentiation and apoptosis in human neuroblastoma cells, Biochem. Biophys. Res. Commun. 351 (2006) 192–197, https://doi.org/10.1016/j.bbrc.2006.10.020.

[25] H. Yoda, T. Inoue, Y. Shinozaki, J. Lin, T. Watanabe, N. Koshikawa, A. Takatori, H. Nagase, Direct targeting of MYCN gene amplification by site-specific DNA alkylation in neuroblastoma, Cancer Res. 79 (2019) 830–840, https://doi.org/10.1158/0008-5472.Can-18-1198.

[26] O.H. Hald, L. Olsen, G. Gallo-Oller, L.H.M. Elfman, C. Lokke, P. Kogner, B. Sveinbjornsson, T. Flaegstad, J.I. Johnsen, C. Einvik, Inhibitors of ribosome biogenesis repress the growth of MYCN-amplified neuroblastoma, Oncogene 38 (2019) 2800–2813, https://doi.org/10.1038/s41388-018-0611-7.

[27] T.L. Lochmann, K.M. Powell, J. Ham, K.V. Floros, D.A.R. Heisey, R.I.J. Kurupi, M.L. Calbert, M.S. Ghotra, P. Greninger, M. Dozmorov, M. Gowda, A.J. Souers, C.P. Reynolds, C.H. Benes, A.C. Faber, Targeted inhibition of histone H3K27 demethylation is effective in high-risk neuroblastoma, Sci. Transl. Med. 10 (2018), https://doi.org/10.1126/scitranslmed.aao4680.

[28] J.I. Fletcher, D.S. Ziegler, T.N. Trahair, G.M. Marshall, M. Haber, M.D. Norris, Too many targets, not enough patients: rethinking neuroblastoma clinical trials, Nature reviews, Cancer 18 (2018) 389–400, https://doi.org/10.1038/s41568-018-0003-x.

[29] A.D. Durbin, M.W. Zimmerman, N.V. Dharia, B.J. Abraham, A.B. Iniguez, N. Weichert-Leahey, S. He, J.M. Krill-Burger, D.E. Root, F. Vazquez, A. Tsherniak, W.C. Hahn, T.R. Golub, R.A. Young, A.T. Look, K. Stegmaier, Selective gene dependencies in MYCN-amplified neuroblastoma include the core transcriptional regulatory circuitry, Nat. Genet. 50 (2018) 1240–1246, https://doi.org/10.1038/s41588-018-0191-z.

[30] S. Klenke, N. Akdeli, P. Stelmach, L. Heukamp, J.H. Schulte, H.S. Bachmann, The

small molecule Bcl-2/Mcl-1 inhibitor TW-37 shows single-agent cytotoxicity in neuroblastoma cell lines, BMC Canc. 19 (2019) 243, https://doi.org/10.1186/s12885-019-5439-1.

[31] F. Lamers, L. Schild, I.J. den Hartog, M.E. Ebus, E.M. Westerhout, I. Ora, J. Koster, R. Versteeg, H.N. Caron, J.J. Molenaar, Targeted BCL2 inhibition effectively inhibits neuroblastoma tumour growth, Eur. J. Cancer (Oxford, England : 1990) 48 (2012) 3093–3103, https://doi.org/10.1016/j.ejca.2012.01.037.

[32] G. Loor, J. Kondapalli, J.M. Schriewer, N.S. Chandel, T.L. Vanden Hoek, P.T. Schumacker, Menadione triggers cell death through ROS-dependent mechanisms involving PARP activation without requiring apoptosis, Free Radic. Biol. Med. 49 (2010) 1925–1936, https://doi.org/10.1016/j.freeradbiomed.2010.09.021.

[33] W. Lutz, M. Stohr, J. Schurmann, A. Wenzel, A. Lohr, M. Schwab, Conditional expression of N-myc in human neuroblastoma cells increases expression of alpha-prothymosin and ornithine decarboxylase and accelerates progression into S-phase early after mitogenic stimulation of quiescent cells, Oncogene 13 (1996) 803–812.

[34] A. Puissant, S.M. Frumm, G. Alexe, C.F. Bassil, J. Qi, Y.H. Chanthery, E.A. Nekritz, R. Zeid, W.C. Gustafson, P. Greninger, M.J. Garnett, U. McDermott, C.H. Benes, A.L. Kung, W.A. Weiss, J.E. Bradner, K. Stegmaier, Targeting MYCN in neuroblastoma by BET bromodomain inhibition, Cancer Discov. 3 (2013) 308–323, https://doi.org/10.1158/2159-8290.Cd-12-0418.